



Report on 3D resistivity modelling with external constraints

Deliverable 5.8

Report on 3D resistivity modelling with external constraints

Deliverable 5.8

Responsible author: Gylfi Páll Hersir (ÍSOR)

Responsible SP leader: Gylfi Páll Hersir (ÍSOR)

Responsible WP leader: Gylfi Páll Hersir (ÍSOR)

Contributions by: Ásdís Benediktsdóttir (ÍSOR),
Gylfi Páll Hersir (ÍSOR), Knútur Árnason (ÍSOR)
and Arnar Már Vilhjálmsson (ÍSOR)

Work package 5.4

November 2019

Website: <http://www.gemex-h2020.eu>



The GEMex project is supported by the European Union's Horizon 2020 programme for Research and Innovation under grant agreement No 727550

Table of Contents

List of figures	3
List of tables	4
Executive summary	5
1 Introduction	6
2 Deep seated low-resistivity anomalies in the Los Humeros and Acoculco survey areas	7
2.1 Los Humeros	8
2.2 Acoculco	11
3 The resistivity model and the basement rock	14
3.1 Prior model of the Los Humeros geothermal area	14
3.2 The basement	15
3.3 Resistivity of the basement rock	16
3.4 Inversion strategies	17
3.5 Results	17
4 Conclusion	22
5 Acknowledgement	23
6 References	23

List of Figures

Figure 1. The Los Humeros area showing the location of the resistivity soundings and a depth-slice at 1000 m below sea-level through the resistivity model.....	9
Figure 2. Several W-E oriented cross-sections through the resistivity model of Los Humeros.....	11
Figure 3. The Acoculco survey area.....	12
Figure 4. A depth-slice at 250 m below sea-level through the resistivity model of Acoculco and a SW-NE oriented cross-section through the resistivity model	13
Figure 5. A W-E oriented cross-section through the resistivity model of Los Humeros	14
Figure 6. A depth-slice at 2000 m above sea-level through the resistivity model of Los Humeros.....	15
Figure 7. Elevation of the basement in the Los Humeros survey area in m a.sl.	16
Figure 8. Final resistivity model based on 3D inversion of MT data from Los Humeros	20
Figure 9. Final resistivity models based on 3D inversion of MT data from Los Humeros.....	21
Figure 10. Data fit for two MT soundings LH033 and LH053	22

List of Tables

Table 1. RMS misfit using three different starting models in the 3D inversion of MT data	17
---	----

Executive summary

The objective of Deliverable D5.8 within the GEMex project is: *3D inversion and modelling of the MT/TEM data from Los Humeros and Acoculco by application of constraints*. The deliverable is based on revisiting the 3D inversion of the 122 static shift corrected MT sounding data from Los Humeros and 68 from Acoculco. The constraints are based on the recent geoscientific findings within the GEMex project from the two areas including geology, gravity and micro-seismic monitoring.

Several datasets were applied to constrain the resistivity models. One of them is on the depth resolution of MT data. Are the deep seated low-resistivity anomalies “found” in Los Humeros and Acoculco real or are they an artefact when applying an unconstrained 3D inversion of the MT data and how do they relate to other geoscientific results? Secondly, the depth to basement in Los Humeros, based on the recent geological model, was used as a constraint. The constrained and unconstrained inversions are compared and discussed.

Upon removing the deep seated low-resistivity anomalies “found” in the unconstrained inversion and forward calculating the models it is evident that the RMS does not change significantly. Therefore, it is concluded that, although the deep seated low-resistivity anomalies are at the intersection of two main geological fault trends, the resolution of MT data is not sufficient to observe such small bodies.

MT data from Los Humeros were 3D inverted using additional starting models which included the basement according to a recent geological model of Los Humeros. Two inversion schemes were applied, one where the basement was kept fixed (scheme 2) and another one where the resistivity within the basement was allowed to change during the inversion (scheme 1). Indications of the deep seated low-resistivity anomaly is present in the final model in scheme 1 but not in scheme 2. Upon looking at what caused the deep seated low-resistivity anomaly it was evident that either regional noise source is causing soundings within a diameter of 2 km to have the same characteristics, a slightly lower apparent resistivity at longer periods, or the anomaly is simply a real signal.

1 Introduction

This report is Deliverable D5.8 within the GEMex project. In the DoW for the project, it says on Deliverable D5.8: *Refers to task 5.8. includes revision of resistivity models from D 5.2 by application of constraints from other data like geological and seismological data. It should result in improved resistivity models.* The task which is referred to here is actually task 5.4.1: *3D inversion and modelling of MT/TEM data from Los Humeros and Acoculco by application of constraints.*

Deliverable D5.2, *Report on resistivity modelling and comparison with other SHGS* describes the data acquisition, processing and 1D and 3D inversion of the resistivity data collected in Los Humeros and Acoculco (GEMex, 2019a). A total of 122 MT and 120 co-located TEM soundings were performed in Los Humeros and 68 MT and 65 co-located TEM soundings in Acoculco.

Data acquisition took place from November 2017 to February 2019. The acquisition period was longer than anticipated because of various problems. However, in the end almost all the planned sites were visited, and the quality of the data was excellent for most of the soundings despite the electromagnetic noise from the power plant in Los Humeros and the associated power lines.

The MT data for both areas were processed and quality controlled. The dimensionality of the data and geoelectrical structure of the areas were analysed through phase tensor analysis and strike analysis. The Los Humeros survey area is characterized by a three-dimensional resistivity structure with considerable horizontal contrast in resistivity. The resistivity structure appears to be characterized by horizontal layers in the Acoculco survey area, with small variations in the lateral directions.

Resistivity models of the two areas were compiled from the results of 1D joint inversion of the TEM and MT data. The MT data used in the inversion were the apparent resistivity and phase calculated from the determinant value of the MT impedance tensor. During the inversion process the MT data were static shift corrected using the TEM data. In Los Humeros the resistivity structure is complex. One of the most prominent feature of the model is a resistive core that domes up along one of the main faults in the region. In Acoculco the resistivity structure is very close to a horizontally layered structure. A conductive cap is revealed at a shallow depth close to a major fault intersection in the area, an area of probable geothermal utilization.

Resistivity models for the two areas were also calculated through 3D inversion of the static shift corrected MT data. For Los Humeros an inversion was done for the full impedance tensor – all 4 complex elements while for Acoculco it was inverted for the off-diagonal elements of the impedance tensor. The WSINV3DMT code (Siripunvaraporn et al., 2005; Siripunvaraporn and Egbert, 2009) was used for the inversion. Four different initial models were used in the inversion for Los Humeros and three for Acoculco. The results from Los Humeros and Acoculco are in good agreement with the 1D inversion results, although the structure in the models became clearer. The resistivity structure in Los Humeros is controlled by the faults in the area as well as the outlines of the Los Potreros caldera. Two main zones of interest were identified. In Acoculco the results are very similar to the 1D joint inversion results, which is not surprising given the horizontally layered structure in the survey area.

Inversion of MT data using external constraints was a part of IMAGE, the EU Horizon 2020 research and innovation programme (IMAGE, 2017). Two different constraints were applied in the study. On one hand the thickness of the low-resistivity cap, as observed from borehole data, was build into the starting model, giving the program a headstart into gaining information on the resistivity in the survey area. On the other hand information on the ductile-brittle bounday was used to infer the location of a deep seated low-resistivity anomaly, which was put into the starting model of the inversion.

Since Deliverable D5.2 became available, a Deliverable on gravity data modelling including a density model has been published for both areas (GEMex, 2019b) and a geological model (GEMex, 2019d) and the seismic structure and various seismological results from the Los Humeros area based on the recording of 45 seismic stations (20 SP and 25 BB) for a period of one-year (GEMex, 2019c). Almost no seismic activity was recorded in Acoculco.

In this work several datasets were applied to constrain the resistivity models. Two of them are discussed here. The first one is on the depth resolution of MT data – are the deep seated low-resistivity anomalies “found” in Los Humeros and Acoculco real or are they an artefact, do they relate to other geoscientific results? In the second one the depth to basement in Los Humeros, based on the recent geological model, is used as a constraint. The resistivity in the basement is calculated and kept as a fixed parameter. Constrained and unconstrained inversion are then compared and discussed.

2 Deep seated low-resistivity anomalies in the Los Humeros and Acoculco survey areas

In this section the depth penetration of electromagnetic-waves (EM-waves) in relation to the sensitivity of MT soundings in high temperature geothermal systems is discussed, addressing the problem of localized deep seated low-resistivity anomalies. These were apparent in the resistivity models in the middle of the survey areas of both Los Humeros and Acoculco. The problem discussed is twofold:

1. The fact that the EM-wave is dissipated in the resistivity structure of high temperature geothermal areas.
2. Long wavelengths are sensitive to structures of a broad scale.

It has been the claim of several authors that the sensitivity of MT data is tens or even hundreds of kilometres. This statement might be true for regions where the resistivity structure is dominated by resistive features. High temperature geothermal areas are, however, characterized by a thick (a few hundred meters) low-resistivity cap underlain by a resistive core (e.g. Árnason, 1987). As the electromagnetic waves penetrate the Earth, a large portion of the energy of the wave is taken up or reflected by the conductive layer, leaving little to penetrate deeper, compared to if the layer was resistive. This behaviour is best depicted in the equation for the skin-depth of the EM-wave (in kilometres);

$$\delta = 0.5 \sqrt{\frac{\rho}{f}}$$

where ρ is the resistivity of the Earth and f is the frequency of the wave. The higher the resistivity of penetrated subsurface is and the lower the frequency, the larger is the skin-depth.

High frequency waves give information about the shallow resistivity structure, as the skin-depth formula shows. The high frequencies also have lateral extent that is proportional to their wavelength. Therefore, the lower the frequency is, the larger is the lateral sensitivity of the wave.

In terms of resistivity models, the shallower parts are better resolved because of the relation between the sensitivity of the wave and its wavelength. The different anomalies imaged at shallow depths are, therefore, better resolved than anomalies in the deeper parts of the model.

In a synthetic resistivity modelling done within the IMAGE project (IMAGE, 2017), data from boreholes were used to constrain the low-resistivity cap. The conclusion was that by interpolating the low-resistivity cap between boreholes a starting model for an inversion could be generated. By doing this, an external dataset was used to constrain the inversion.

How is it possible to constrain the inversion in the deeper parts of the model where the uncertainty is greater? This question has been in the discussion for quite some time and is important because of the limited resolution of geophysical data sets at a great depth.

Therefore, this is at the core of the problem faced in resistivity modelling in Los Humeros and Acoculco. How can one be sure that the deep seated low-resistivity anomalies are not an artefact of the modelling?

The following sub-sections describe the deep localized low-resistivity anomalies that appeared in the resistivity models of Los Humeros and Acoculco. Their location relative to other datasets is discussed and arguments on whether the anomalies are true or artefacts. The deep-seated low-resistivity anomaly is also mentioned in Section 3.

2.1 Los Humeros

A resistivity model of Los Humeros based on 3D inversion of MT data is presented in Deliverable 5.2 of the GEMex project (GEMex, 2019a). The resistivity structure of the Los Humeros system exhibits the typical structure of a high temperature geothermal system. A low-resistivity cap domes up and is underlain by a resistive core.

Figure 1A shows the location of TEM/MT soundings in the survey and the main geological features and Figure 1B shows a horizontal slice through the resistivity model at 1000 m below sea level. A circle marked with red dashed lines outlines the location of the deep seated low-resistivity anomaly. The question here is: Is this anomaly real or is it an artefact produced by the inversion code? At ÍSOR the experience based on 3D inversion in several areas, indicates that an artefact like this one – low-resistivity bubble at considerable depth – often emerges although physically it cannot be resolved (see e.g. Lee et al., 2019).

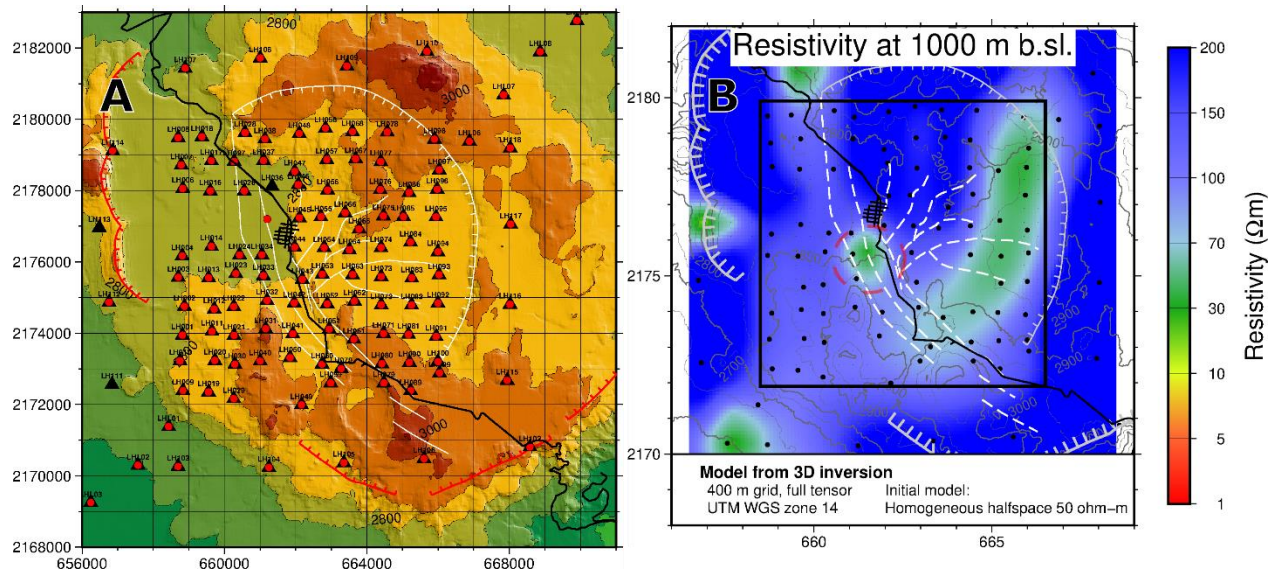


Figure 1. A: The Los Humeros area showing the location of the resistivity soundings; black triangles and red dots are MT and TEM soundings, respectively. Red and white lines with ticks are the Los Humeros and Los Potreros calderas, respectively. White lines are major faults in the area and black lines are roads. The Los Humeros town is in the middle of the survey area, denoted by a net of roads. Coordinate system is UTM zone 14 WGS84 in km. **B.** A depth-slice at 1000 m below sea-level through the resistivity model of Los Humeros based on 3D inversion of MT data (GEMex, 2019a). The black square is the area of the dense grid of the model and black dots are MT soundings. A circle marked with red dashed lines outlines the deep seated low-resistivity anomaly.

The deep seated low-resistivity anomaly extends from about 1000 m below sea level down to about 6000 m below sea level (Figure 2B). The maximum lateral extent of the anomaly is 1.5 km x 1.5 km. The location of the anomaly with respect to the geology is interesting as it is located where two fault trends join. Therefore, one might claim that the location of the anomaly is not randomness since it coincides with geological evidences.

Micro-seismic activity in Los Humeros was monitored for a period of one year within GEMex using 45 seismic stations (20 short-period (SP) and 25 broadband (BB) seismometers) as a part of detecting the deep structures (GEMex, 2019c). Earthquake locations have been plotted on the resistivity cross-sections in Figure 2. Interestingly, the western seismic swarm that is located above the deep seated low-resistivity anomaly (located at approximately $x=-1$ km), is a few hundred meters shallower than the swarm to the east (located at $x=1.5$ km). Is that an indication of an up-flow area, reducing the depth to the brittle-ductile boundary above the deep seated low-resistivity anomaly? The nature of the two swarms are of separate origin; the swarm to the west is related to injection of geothermal fluids back into the system but the eastern swarm is composed of naturally occurring earthquakes (GEMex, 2019c). The injection-related swarm could be limited by the depth of the injection wells whereas the naturally occurring earthquakes are a better representation of the brittle-ductile boundary.

Lee et al. (2019) undertook a resolution test to evaluate the sensitivity of MT data to the size, shape, resistivity value and location of an upper crustal magma body. They tested three shapes including a cube, with each side of 1 km, underneath the Krafla geothermal area in Iceland at a depth of 1.6 km b.sl. (2.1 km below surface). Rhyolite magma was encountered at that depth during drilling of well IDDP-1, which was the reason for the chosen depth. Lee et al. (2019) tested 6 resistivity values in the range of 0.1 Ωm to 30 Ωm and compared statistically the calculated response to the response of a model that did not contain the cube. The results were that, for all resistivity values, the two models with and without the cube, were statistically the same.

The study of Lee et al. (2019) in Krafla showed that even a 1 km³ magma body at 2.1 km depth below surface could not be resolved. The geothermal system in Krafla exhibits a rather thick low-resistivity cap, which Lee et al. (2019) regarded as the main reason for that the magma body was not detected.

There is a difference between the size parameter of the low-resistivity body in the Krafla resolution experiment and the deep seated low-resistivity anomaly at Los Humeros which is; the anomaly at Los Humeros is a 4 km tall and 1.5 km wide cylinder; a volume of around 7 km³.

In order to explore if the deep seated low-resistivity anomaly influences the misfit, the anomaly was removed from the resistivity model and the corresponding data forward calculated. The normalized RMS misfit including the deep seated low-resistivity anomaly was 1.23 while the RMS misfit not including the anomaly was 1.27. The difference in RMS is not large and hardly statistically significant, but one might claim that the model *with* the anomaly would be the model preferred. However, the difference is very subtle and upon examining the fit of the stations close-by for the two models, the RMS fit is either a little bit better or a little bit worse.

Upon removing the anomaly and replacing intermediate resistivity values, the inversion was kept running. After two iterations the anomaly was back at the same location as it had been before. In hindsight it might have proved a good test to insert very large resistivity values in order to see if the data required that the model included the low-resistivity anomaly or not.

To conclude, it was decided to remove the anomaly on the basis of limited resolution at depth, while keeping in mind that the anomaly might be 'true' and if so then it is representing an interesting body to explore, in particular its convergence with the geology.

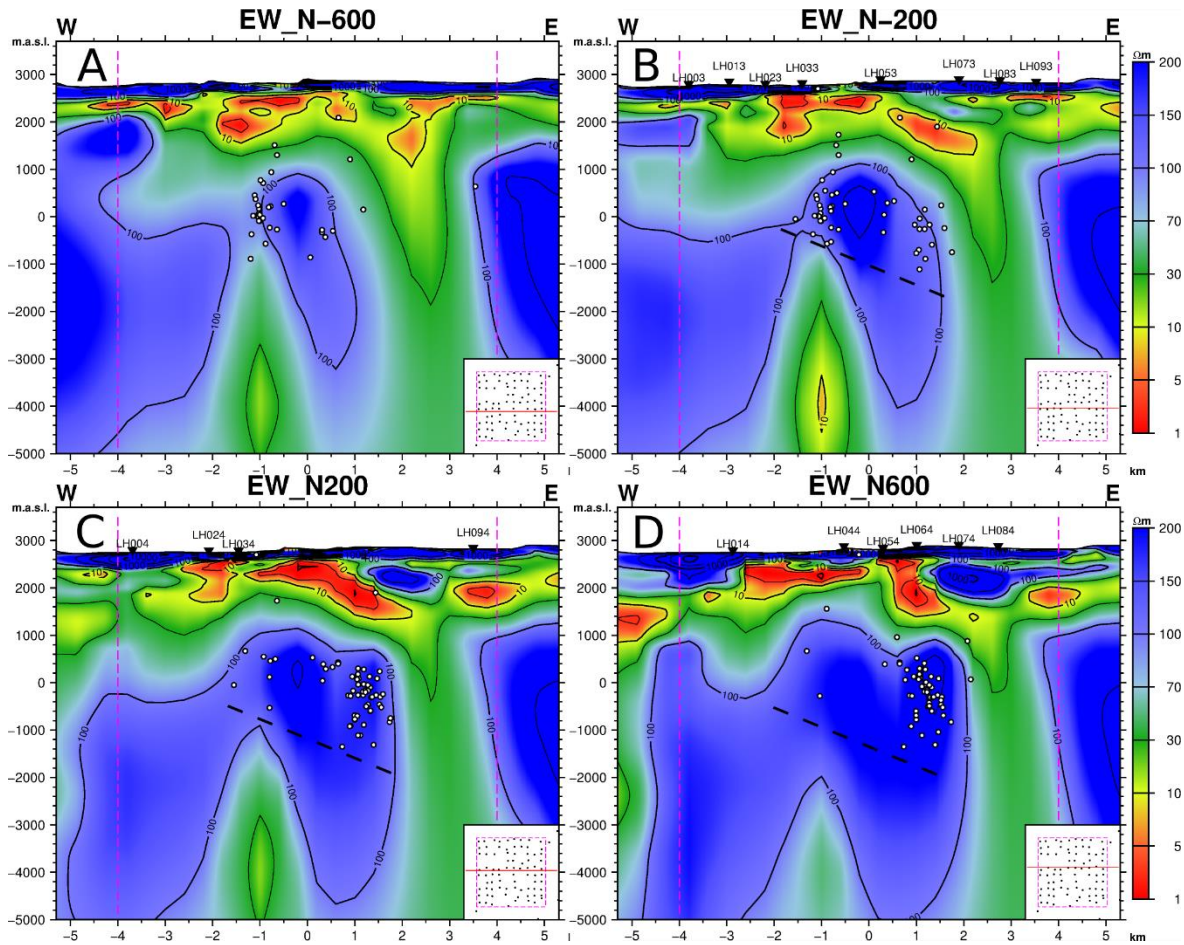


Figure 2. Several W-E oriented cross-sections through the resistivity model of Los Humeros based on 3D inversion of MT data (GEMex, 2019a), running from south (A) to north (D). The densely gridded area is within the dashed pink lines. Sounding locations are shown as inverted triangles at the surface with their name. Dots are earthquake locations (GEMex, 2019c). The deep seated low-resistivity anomaly is seen at $x=-1$ km and at a depth of -1000 m to -5000 m. The dashed black line emphasizes the depth difference between the western and eastern seismic swarms. Small inlet in the bottom right corner: Location of the cross-section shown as a red line relative to the MT-locations (black dots).

2.2 Acoculco

A resistivity model of Acoculco based on 3D inversion of MT data is presented in Deliverable 5.2 of the GEMex project (GEMex, 2019a). The resistivity structure of the Acoculco system exhibits a typical structure of a high temperature geothermal system. A low-resistivity cap underlain by a resistive core. The data coverage in Acoculco was less extensive than in Los Humeros and did not cover the whole of the Acoculco caldera.

Figure 3 shows the survey area and the main geological features of the area and Figure 4 shows a depth-slice at 250 m below sea level and a cross-section through the resistivity model of Acoculco.

The deep seated low-resistivity anomaly extends from about 800 m below sea level down to about 4000 m below sea level (Figure 4B). The maximum lateral extent of the anomaly is around 1 km x 1 km. Like the deep seated low-resistivity anomaly in Los Humeros, the location of the anomaly with respect to the geology is interesting, as it is located where two fault trends join.

The low-resistivity anomaly in Acoculco was also removed from the model. The RMS of the model with and without the anomaly was 1.26 in both cases. When continuing the inversion, the deep seated low-resistivity anomaly did not reappear.

In conclusion for the Acoculco model, it was decided to remove the deep seated low-resistivity anomaly due to limited depth resolution.

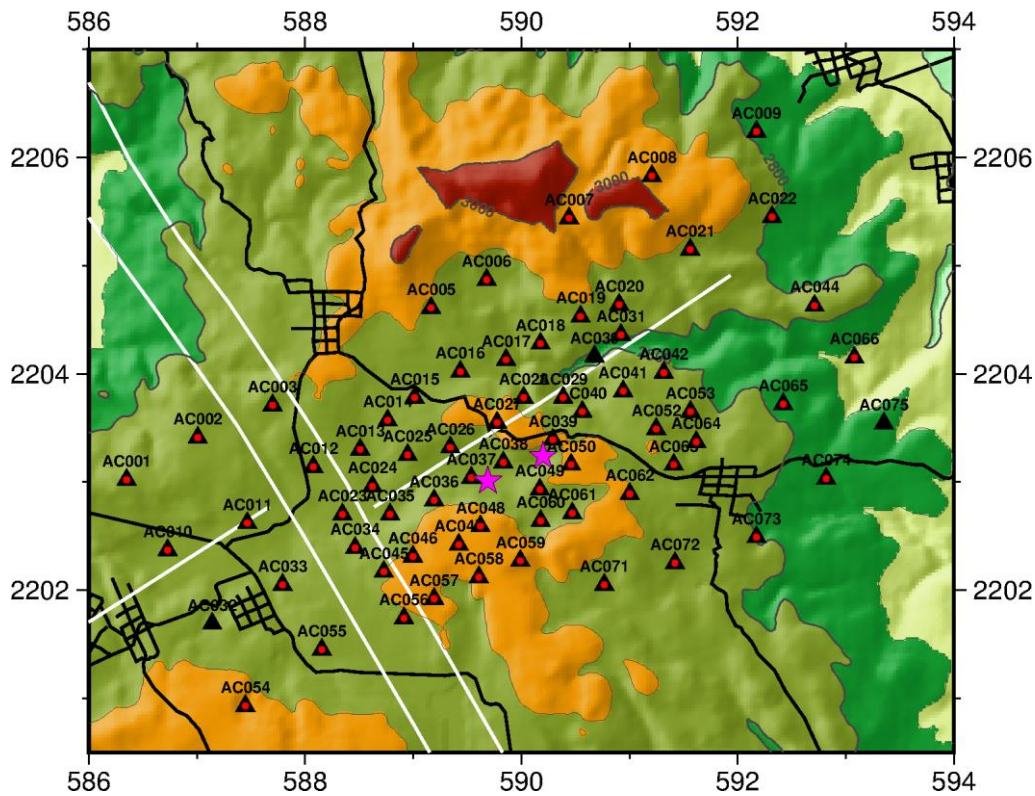


Figure 3. The Acoculco survey area. Black triangles and red circles denote the location of the MT and TEM soundings, respectively. White lines are major faults in the area, black lines are roads, and magenta stars are wells EAC 1 and 2. Coordinate system is UTM zone 14 WGS84 in km.

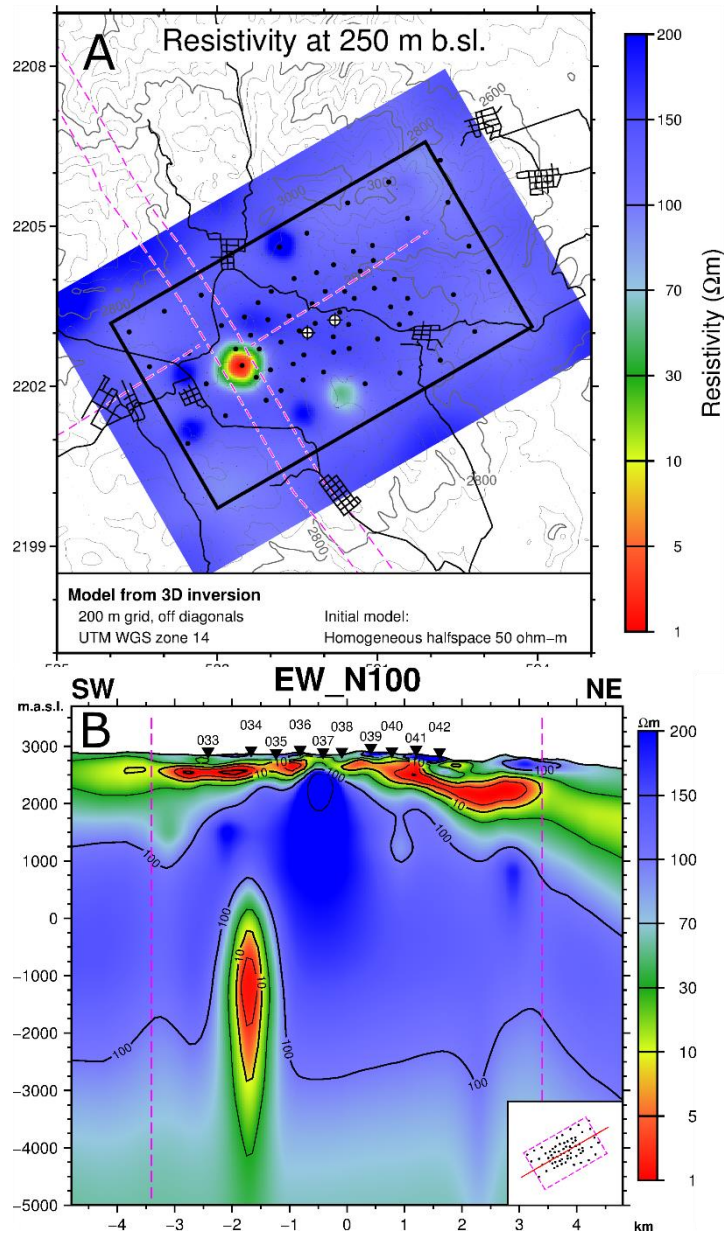


Figure 4. **A.** A depth-slice at 250 m below sea-level through the resistivity model of Acoculco based on 3D inversion of MT data (GEMex, 2019a). Black dots are MT sites. The black box outlines the densely gridded area in the inversion. Dark gray lines are roads, gray lines are elevation contours and pink dashed lines are the main faults in the region. The two black crosses on white circles are the two EAC wells. **B.** A SW-NE oriented cross-section through the resistivity model of Acoculco (GEMex, 2019a). The densely gridded area is within the dashed pink lines. Sounding locations are shown as inverted triangles at the surface with their name. The deep seated low-resistivity anomaly is seen at $x = -1.8$ km and at a depth of 800 m to -4000 m. Small inset in the bottom right corner: Location of the cross-section shown as a red line relative to the MT-locations (black dots).

3 The resistivity model and the basement rock

This section describes how the basement from a geological model was used to constrain the inversion of the MT data from Los Humeros.

3.1 Prior model of the Los Humeros geothermal area

3D inversion of MT data is a highly underdetermined problem, i.e. the number of unknown resistivity values is much bigger than the number of data values. The iterative 3D inversion is started from an initial or a starting model. In order to help regularize the inversion, a prior model is used to constrain the deviation of the resulting model from the prior model as discussed in Deliverable D5.2 (GEMex, 2019a). Consequently, the resulting model may depend on the initial and prior model which in this case are the same.

A 3D resistivity model for Los Humeros is presented in Deliverable 5.2 of the GEMex project (GEMex, 2019a). The model showed a resistivity structure typical of a geothermal system in volcanic region, with an up-doming low-resistivity cap underlain by a resistive core. The uppermost few km of the resistivity model fit quite to some extent with the geology of the area, i.e. faults within the western part of the Los Humeros caldera (see Figures 5 and 6). A vertical low-resistivity anomaly is revealed below MT sounding LH023 and LH033 as seen on Figure 5. LH033 is located at the Antigua fault (see Figure 1).

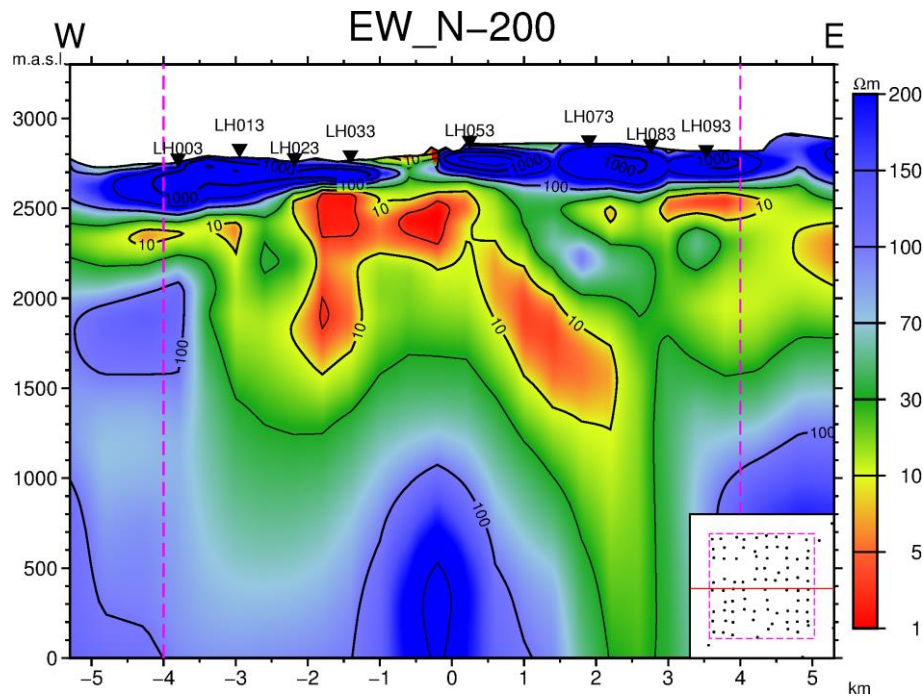


Figure 5. A W-E oriented cross-section through the resistivity model of Los Humeros based on 3D inversion of MT data (GEMex, 2019a). The densely gridded area is within the dashed pink lines. Sounding locations are shown as inverted triangles at the surface with their name. Small inlet in the bottom right corner: Location of the cross-section shown as a red line relative to the MT-locations (black dots).

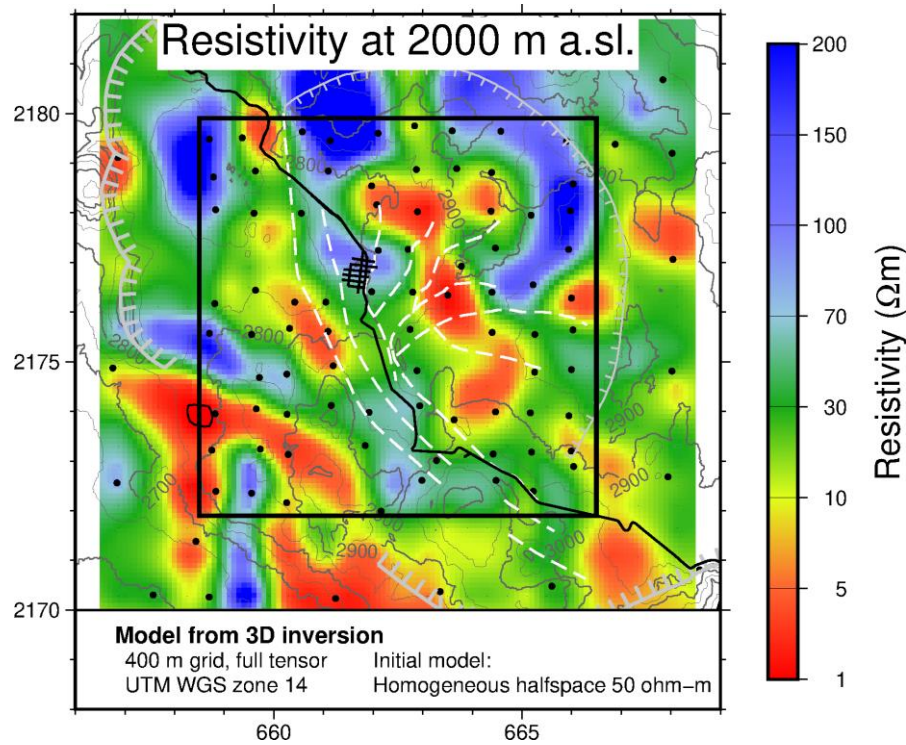


Figure 6. A depth-slice at 2000 m above sea-level through the resistivity model of Los Humeros based on 3D inversion of MT data (GEMex, 2019a). The black square is the area of the dense grid of the model and black dots are MT soundings. Grey thick and thin lines with ticks are the Los Humeros and Los Potreros calderas, respectively. White lines are major faults in the area and black lines are roads. The town of Los Humeros is located in the middle of the survey area, denoted by a net of roads. Coordinate system is UTM zone 14 WGS84.

It is more complicated to interpret the deeper part of the resistivity model (> 3 km depth) as the resolution of MT soundings diminishes greatly with depth. The starting model in the 3D inversion of the MT data from Los Humeros shown here was a 50 Ωm homogeneous half-space (GEMex, 2019a). The inversion was unconstrained by other datasets, resulting in some far-away low-resistivity anomalies in the large padding cells in the modelling grid. This characteristic of the model has been observed in models with the same inversion code (IMAGE, 2017). As in the case of the deep seated low-resistivity anomaly, discussed earlier, it is important to be aware of the limitations of the inversion code used.

3.2 The basement

A local geological model of Los Humeros has been created within Work package 3 of the GEMex project (Calcagno et al., 2018; Calcagno et al., 2020). The model consists of layers of caldera formation, pre-caldera formation and a basement. Here, external dataset is used to constrain the 3D inversion of the MT data, by giving the basement of the geological model, a fixed resistivity value.

Figure 7 shows the topography of the basement according to Calcagno et al. (2018) and Calcagno et al. (2020). The top of the basement varies in elevation and reaches highest elevation at 2055 m above sea

level and lowest at 750 m below sea level. The local geological model of Los Humeros has smaller extent than the model grid used in the inversion of the MT data and smaller than the elevation grid, used to elevate-correct the model. The 3D model grid extends far out, outside both the geological model as well as the elevation grid. Therefore, the elevation of the basement outside the bounds of the local model was set to the mean elevation of the basement, 750 m above sea level and further outside the bounds of the elevation grid, the basement was fixed at 4500 m below the surface (around 2000 m below sea level).

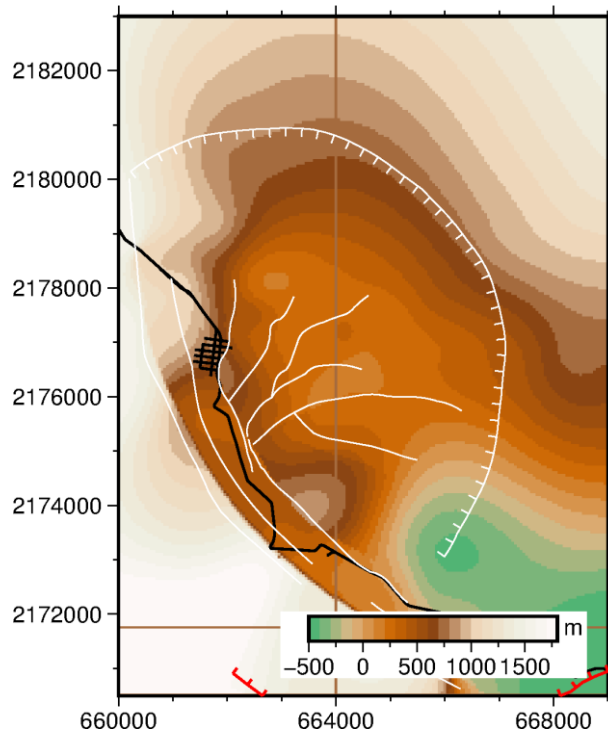


Figure 7. Elevation of the basement in the Los Humeros survey area in m a.s.l. White and red lines with ticks are the Los Potreros and Los Humeros calderas, respectively. White lines are regional faults and black lines are roads.

3.3 Resistivity of the basement rock

The basement rocks in Los Humeros are Mesozoic calcareous and/or granitic rocks. It is assumed that the rock matrix is highly resistive, and that electrical conductivity is mainly due to fluids in pores (fractures) and can be estimated using Archie's law (Archie, 1942) stating that:

$$\sigma_b = \sigma_w \cdot a \cdot \phi^m$$

where σ_b and σ_w are the bulk and fluid conductivities, respectively and ϕ is fractional porosity. The constants a and m are generally referred to as tortuosity and cementation factors. Most commonly, a is found to be close to 1 and m in the range of 1 – 2. Mohamad and Hamada (2017) have measured these parameters for carbonate rocks and find a close to 1 and m close to 2.

The conductivity of discharged well fluids in Los Humeros at 25°C is reported to be in the range of 254 to 1295 $\mu\text{S}/\text{cm}$ or $2.54 \cdot 10^{-2}$ to $1.3 \cdot 10^{-1}$ S/m (GEMex, 2019e). Quist and Marshall (1968) have measured temperature dependence of Sodium Chlorite solutions over a wide temperature and pressure range and according to their findings conductivity of the well fluids would increase by approximately a factor of 7, when heated from 25°C to about 350-400°C.

Taking the higher water conductivity value above and $a = 1$ and $m = 2$, and porosity 3% we get an estimate of the basement conductivity:

$$\sigma_b = 7 \cdot 1.3 \cdot 10^{-1} \cdot (0.03)^2 \text{ S/m} = 8.19 \cdot 10^{-4} \text{ S/m} \text{ i.e. resistivity } \rho_b = 1.22 \cdot 10^3 \Omega\text{m}$$

We have, therefore, assumed that the resistivity of the basement rock to be of the order of magnitude of $10^3 \Omega\text{m}$.

3.4 Inversion strategies

Two inversion schemes were adopted in this work;

1. A starting model including the basement with a resistivity value of 1000 Ωm and the rest of the model space with 50 Ωm . In the inversion the resistivity of the basement was not fixed, resistivity in all cubes could be changed during the inversion.
2. A starting model including the basement with a resistivity value of 1000 Ωm and the rest of the model space with 50 Ωm . The resistivity in the basement was kept fixed during the inversion, the resistivity in the cubes above the basement were changed during the inversion.

In both inversion schemes the background value of 50 Ωm was chosen since the final model of Los Humeros, presented in Deliverable 5.2 (GEMex, 2019a), had a homogeneous half-space of 50 Ωm as the starting model.

3.5 Results

Table 1 summarizes the RMS of the final misfit of the 3D inversion of MT data using three different starting models, the one given in Deliverable 5.2 (GEMex, 2019a) and from inversion scheme 1 and 2. At 8 iterations the unconstrained model showed a better fit, compared to the constrained versions. This is not a surprise since there are no constraints on what the code can do.

Table 1. *RMS misfit using three different starting models in the 3D inversion of MT data*

Model	RMS	Number of iterations
Unconstrained model	1.27 (1.44)	15 (8)
Model from inversion scheme 1	1.49	8

Model from inversion scheme 2	2.9	8
-------------------------------	-----	---

Figure 8 shows resistivity depth-slices from the original model (Deliverable 5.2; GEMex, 2019a) and the resulting models from inversion schemes 1 and 2.

Figure 8 A-C shows a depth-slice at 25 km below the surface. This depth is beyond the resolution depth of the MT data, but still the inversion code sticks in low-resistivity anomalies. For the unconstrained model a large low-resistivity anomaly is present in the southwestern corner of the model space and in cells close to the dense central part of the grid (Figure 8 A). The smaller low-resistivity anomaly is present in the model from inversion scheme 1 (Figure 8 B). The area around the dense part of the grid does not exhibit as many low-resistivity anomalies as in the unconstrained model. In the model from inversion scheme 2 no anomaly is present at this depth as it is in the fixed part of the model space.

At 2200 m a.sl. (Figure 8 D, E, F) the three models are the same. This is not surprising since the constraints in the models are well below the depth-slice. At sea level, the model with the basement pre-set in the initial model (scheme 1) and the model with fixed basement (scheme 2) show different structure than the original unconstrained model. The unconstrained model exhibits a low-resistivity structure (Figure 8 G). This anomaly is not present in the models from scheme 1 and 2 (Figures 8 H, I). The fact that the low-resistivity anomaly does not arise in the model from inversion scheme 1 tells that the inversion results are strongly dependent on the starting model of the inversion. At this depth most of the densely gridded area of the inversion is in the basement, perhaps aside the south-eastern corner of the densely gridded area (Figure 7).

At 2000 m b.sl. the deep seated low-resistivity anomaly, discussed in Section 2, is present in both the unconstrained model and model resulting from inversion scheme 1. It is not present in the model from inversion scheme 2, as the resistivity in this part of the model space was fixed with 1000 Ωm .

Figure 9 shows the same W-E oriented resistivity cross-section through the original model from Deliverable 5.2 (Figure 9 A) and the resulting models from inversion scheme 1 (Figure 9 B) and scheme 2 (Figure 9 C). The deep-seated low-resistivity anomaly is present in the unconstrained model and the model from scheme 1. The anomaly is not as pronounced in the model from scheme 1 as in the unconstrained model, but it is still present. The anomaly is located where the starting model value was 1000 Ωm . Does this mean that the anomaly is real, as it appears even though the initial model was two orders of magnitude larger than the resistivity value of the anomaly?

In order to further examine the existence of the deep seated low-resistivity anomaly, it is of interest to inspect the data fit of two soundings (Figure 10) that are located above the deep seated low-resistivity anomaly, station LH033 and LH053 (for location of the soundings see Figure 1 and Figure 9).

MT sounding LH033 does not have long enough periods to be able to image the deep seated anomaly. The data in sounding LH053 show that there is a change in the apparent resistivity at around a period of 30 s,

with a significantly decreasing apparent resistivity, indicating a deep seated low-resistivity body below the sounding side.

Sounding LH034, LH041, LH052 and LH045 show a decreasing apparent resistivity for both polarizations at long periods (20 s -100 s) and for one polarization in sounding LH044 and LH054 (the other polarization has bad data).

If there is a noise source in the area causing the observed tendency in the soundings, exhibiting a lower resistivity value at longer periods, then it is a wide-spread noise source as these soundings cover an area with a diameter of roughly 2 km. The quality of the long period data was generally of worse than for the short period data.

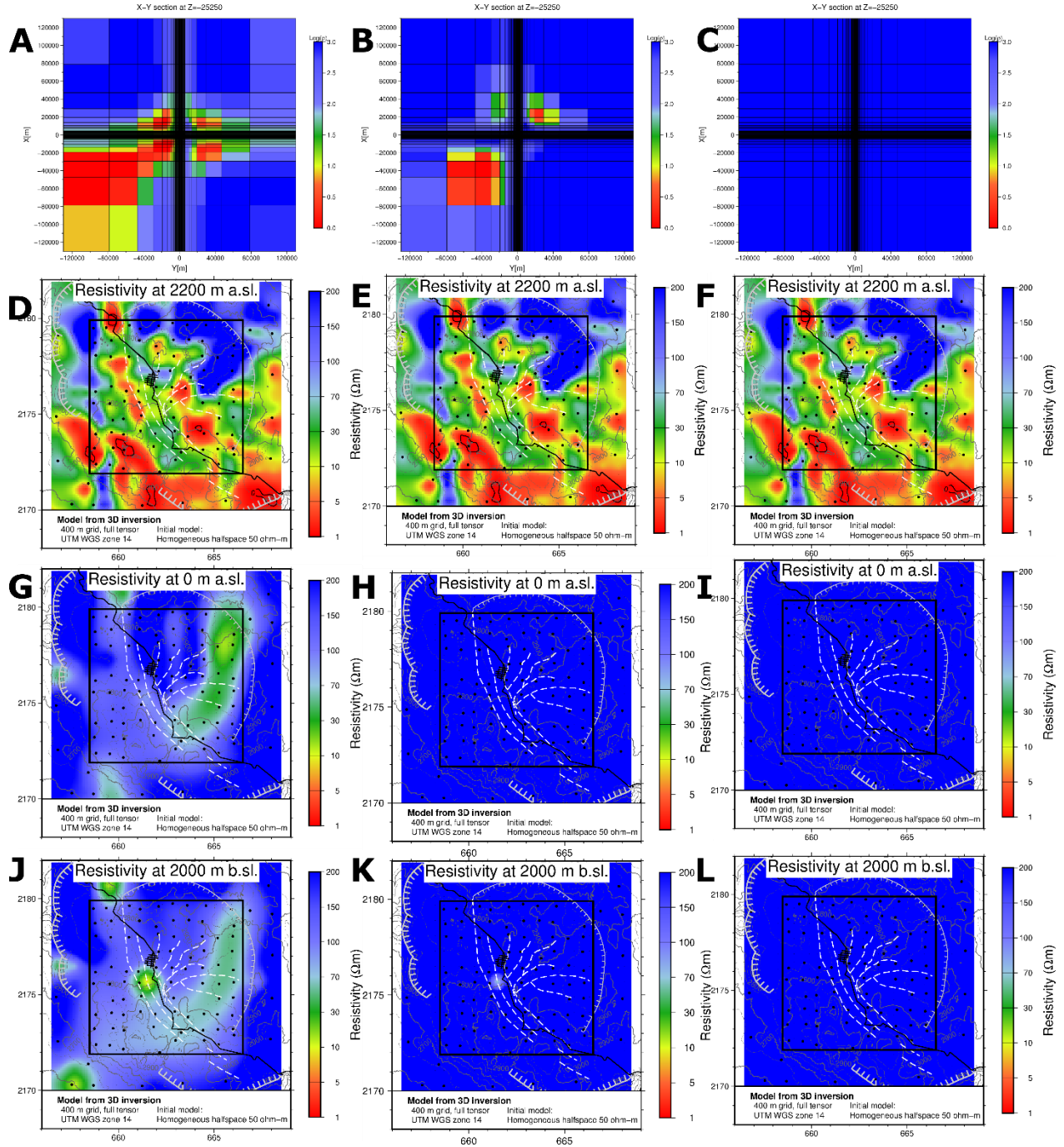


Figure 8. Final resistivity model based on 3D inversion of MT data from Los Humeros presented as depth-slices using three different starting models. The left column is the unconstrained inversion (Deliverable D5.2), in the middle is scheme 1 and the right column is scheme 2. The uppermost panel (A, B and C) shows a depth-slice at 25250 m below surface showing the whole grid space. The other panels show depth-slices at 2000 m a.s.l. (D, E and F), at sea level (G, H and I) and at 2000 m b.s.l (J, K and L), respectively. For figure legend, see Figure 6.

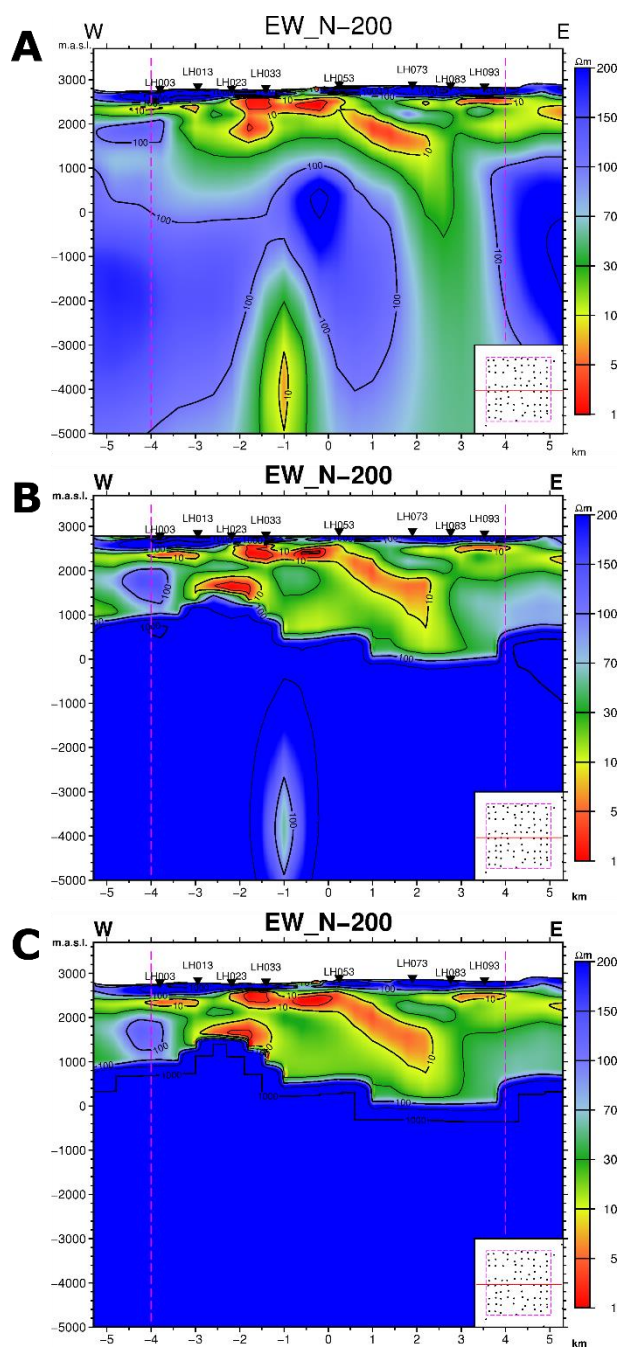


Figure 9. Final resistivity models based on 3D inversion of MT data from Los Humeros presented as cross-sections at the same location using three different starting models. **A:** Unconstrained inversion (Deliverable D5.2). **B:** Scheme 1 and **C:** Scheme 2. For figure legend, see Figure 5.

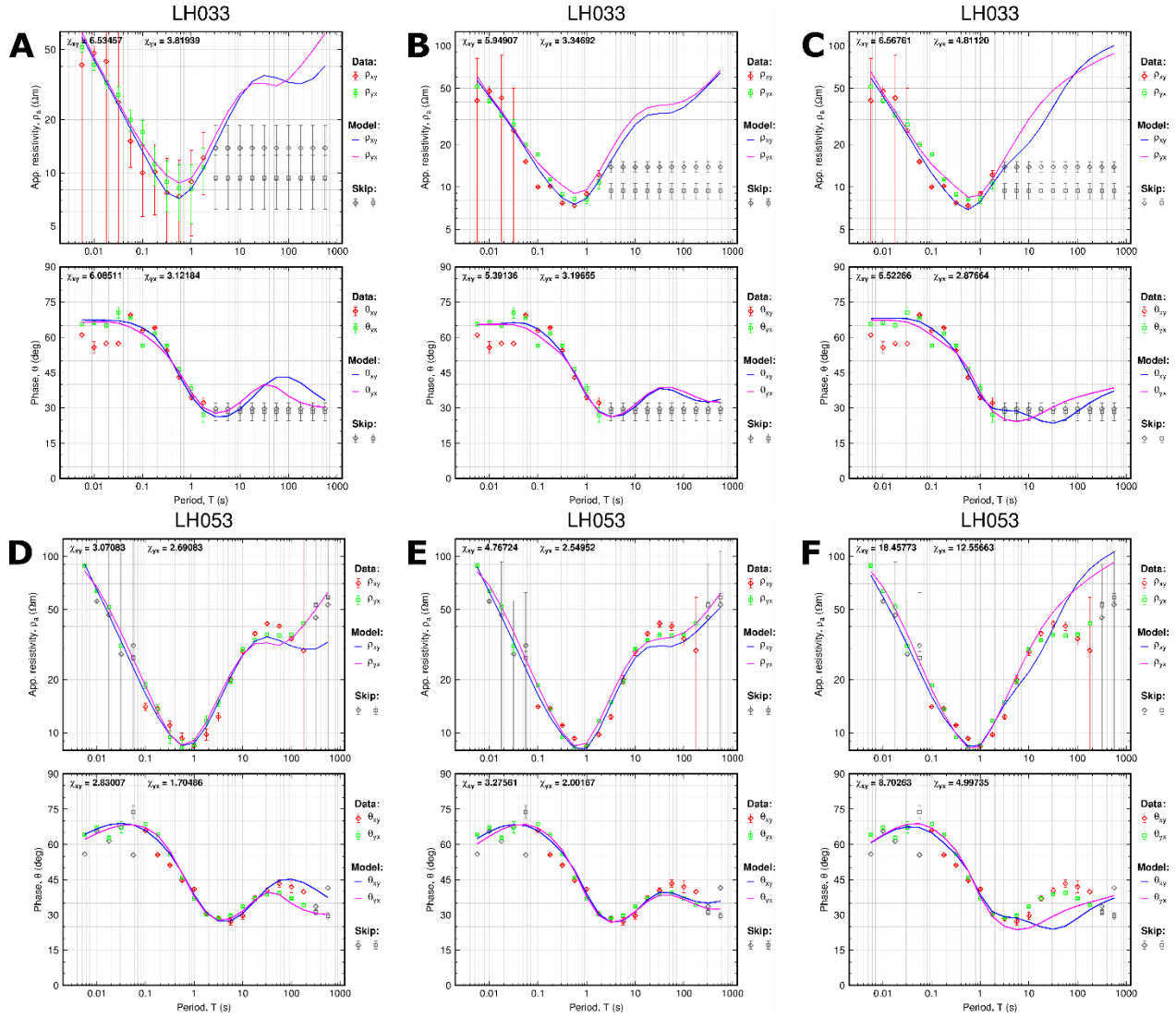


Figure 10. Data fit for two MT soundings LH033 and LH053, for location, see Figure 1 and 9. The left column are data from the unconstrained inversion (Deliverable D5.2), in the middle from scheme 1 and the right column shows MT data from scheme 2.

4 Conclusion

The resistivity models of Los Humeros and Acoculco survey areas have been refined by:

1. Investigating deep seated low-resistivity anomalies with respect to other datasets, i.e. geological structures and micro-earthquakes. Furthermore, the resolution of MT data is discussed and upon removing the anomalies and forward calculating the models finding that the RMS did not change

significantly. Therefore, it is concluded that, although the deep seated low-resistivity anomalies are at the intersection of two main fault trends, the resolution of MT data is not sufficient to observe such small bodies.

2. Inverting the MT data from Los Humeros using other starting models. The additional starting models included the basement according to a recent geological model of Los Humeros. Two inversion schemes were applied, one where the basement was kept fixed (scheme 2) and another one where the resistivity within the basement was allowed to change during the inversion (scheme 1). Indications of the deep seated low-resistivity anomaly is present in the final model in scheme 1 but not in scheme 2. Upon looking at what caused the deep seated low-resistivity anomaly it was evident that either regional noise source is causing soundings within a diameter of 2 km to have the same characteristics, a slightly lower apparent resistivity at longer periods, or the anomaly is simply a real signal.

5 Acknowledgements

The authors wish to thank the Comisión Federal de Electricidad (CFE, Mexico) for their assistance and support. We also wish to thank our collaborators in the Mexican consortium, UNAM (National Autonomous University of Mexico), UMSNH (Michoacan University of Saint Nicholas of Hidalgo, Mexico) and CISESE (Ensenada Centre for Scientific Research and Higher Education, Mexico) as well as KIT (Karlsruhe Institute of Technology, Germany) from the European consortium for their participation in the field work and processing and inversion of the resistivity data and not the least the fruitful discussions on the interpretation of the data. Special thanks go to Claudia Arango Galván at UNAM.

6 References

- Archie, R.G., 1942: The electrical resistivity log as an aid in determining some reservoir characteristics. *Trans. AIME*, 146, 54-67.
- Árnason, K., Flóvenz, Ó.G., Georgsson, L.S. and Hersir, G.P., 1987: Resistivity structure of high temperature geothermal system in Iceland. *International Union of Geodesy and Geophysics (IUGG) XIX General Assembly*. Vancouver, Canada, Abstract V, 477.
- Calcagno, P., Evanno, G., Trumpy, E., Gutiérrez-Negrín, L.C., Macías, J. L., Carrasco-Núñez, G. and Liotta, D. 2018: Preliminary 3-D geological models of Los Humeros and Acoculco geothermal fields (Mexico)– H2020 GEMex Project. *Advances in Geosciences*, 45, 321-333.
- Calcagno, P., Trumpy, E., Gutiérrez-Negrín, L.C., Norini, G., Macías, J.L., Carrasco-Núñez, G., Liotta, D., Garduño-Monroy, V.H., Hersir, G.P., Vaessen, L., Evanno, G. and Arango Galván, C., 2020. Updating the 3D Geomodels of Los Humeros and Acoculco Geothermal Systems (Mexico) – H2020 GEMex Project. In: *Proceedings of the World Geothermal Congress 2020 Reykjavík, Iceland*.
- GEMex, 2019a. GEMEX-Deliverable D5.2: *Report on resistivity modelling and comparison with other SHGS*. <http://www.gemex-h2020.eu>, 157 pp.
- GEMex, 2019b. GEMEX-Deliverable D5.6: *Report on gravity modelling*. <http://www.gemex-h2020.eu>, 157 pp.

- GEMex, 2019c. GEMEX-Deliverable D5.3: *Seismic structures of the Acoculco and Los Humeros geothermal fields*. <http://www.gemex-h2020.eu>, 129 pp.
- GEMex, 2019d. GEMEX-Deliverable D4.1: *Final report on active systems: Los Humeros and Acoculco*. <http://www.gemex-h2020.eu>, 334 pp.
- GEMex, 2019e. GEMEX-Deliverable D4.3: *Final Report on geochemical characterization and origin of cold and thermal fluid*. <http://www.gemex-h2020.eu>, 213 pp.
- IMAGE, 2017. IMAGE-D5.6: *MT-Inversion techniques with external constraints*. (GA-608553). *Seventh Framework Programme*, 63 pp.
- Lee, B., Unsworth, M., Árnason, K. and Cordell, D., 2019. Imaging the magmatic system beneath the Krafla Geothermal field, Iceland: A new 3-D electrical resistivity model from inversion of magnetotelluric data. *Geophysical Journal International*.
- Mohamad, A., M. and Hamada, G. M., 2017. Determination techniques of Archie's parameters: a, m and n in heterogeneous reservoirs. *Journal of Geophysics and Engineering*. Volume 14, Issue 6, December 2017, 1358–1367.
- Quist, A.S. and Marshall, W.L., 1968. Electrical Conductance of Aqueous Sodium Chloride Solutions from 0° to 800° and Pressure to 4000 Bars. *The Journal of Geophysical Chemistry*. Vol. 72, Number 2, February 1968, 684-703.
- Siripunvaraporn, W., Egbert, G., Lenbury, Y. and Uyeshima, M., 2005. Three-dimensional magnetotelluric inversion: data-space method. *Phys. Earth Planet. Int.*, 150, no. 1, 3–14.
- Siripunvaraporn, W. and Egbert, G., 2009. WSINV3DMT: Vertical magnetic field transfer function inversion and parallel implementation. *Phys. Earth Planet. Int.*, 173, no. 3, 317–329.



Coordination Office, GEMex project

Helmholtz-Zentrum Potsdam
Deutsches GeoForschungsZentrum

Telegrafenberg, 14473 Potsdam

Germany